*J. Fluid Mech.* (1987), *vol.* 179, *pp.* 283–305
*Printed in Great Britain*



# Large deformations of a cylindrical liquid-filled membrane by a viscous shear flow

By GEORGE I. ZAHALAK, PEDDADA R. RAO AND SALVATORE P. SUTERA

Department of Mechanical Engineering, Washington University, St Louis, MO 63130, USA

(Received 29 July 1986 and in revised form 14 November 1986)

This paper treats the steady flow fields generated inside and outside an initially circular, inextensible, cylindrical membrane filled with an incompressible viscous fluid when the membrane is placed in a two-dimensional shear flow of another viscous fluid. The Reynolds numbers of both the interior and exterior flows were assumed to be zero ('creeping flow'), but no further approximations were made in the formulation. A series solution of the resulting free boundary-value problem in powers of a dimensionless shear rate parameter was constructed through fifth order. When combined with a conformal coordinate transformation this series gave accurate results for large deformations of the membrane (up to an aspect ratio of 2.5). The rather tedious algebraic manipulations required to obtain the series solution were done by computer with a symbol-manipulation program (REDUCE), which both formulated the boundary-value problems for each successive order and solved them. Results are presented which show how the shear rate and fluid viscosities influence the internal and external velocity and pressure fields, the membrane deformation and its 'tank-treading' frequency, and the membrane tension.

This work demonstrates that classical perturbation techniques combined with computer algebra offer a useful alternative to purely numerical methods for problems of this type.

## 1. Introduction

The problem of calculating the deformations produced in a very flexible closed membrane, filled with a viscous liquid, by an external flow of another viscous liquid is of considerable interest in suspension rheology. Further, this problem has assumed importance in biomechanics since the discovery of the 'tank-treading' phenomenon in red blood cells (Schmid-Schönbein & Wells 1969) and the attempt to use this phenomenon for diagnostic purposes (Sutera *et al.* 1985). Thus it is unfortunate that the problem is very intractable from a mathematical viewpoint, as it requires the imposition of complex boundary conditions on an *a priori* unknown surface. Exact solutions are unknown but two lines of attack have yielded useful approximate results. In the first, reasonable *a priori* assumptions are made about the shape and surface velocity of the deformed membrane (Kholief & Weymann 1974; Keller & Skalak 1982; Sutera & Tran-Son-Tay 1983). This results in simplified linear boundary-value problems for the determination of the external and internal flow fields, but at the price of some inconsistency with the membrane constitutive relations which actually determine its shape and surface speed. The only numerical studies of the tank-treading problem published thus far are the finite-element analyses of Niimi & Sugihara (Sugihara & Niimi 1984; Niimi & Sugihara 1985) which assume the form

of the membrane and its velocity, and further are restricted to two-dimensional flow fields.

The second approach follows G. I. Taylor's classic analysis of liquid droplets (Taylor 1932) and attempts to construct a series expansion of the solution in terms of a small parameter measuring the membrane deformation. This type of analysis has been carried furthest in the recent work of Barthes-Biesel, for initially-spherical elastic (Barthes-Biesel 1980) and viscoelastic (Barthes-Biesel & Sgaier 1985) membranes. The main advantage of this boundary-perturbation technique is that no compromises need be made in the correct physical formulation of the problem. But its main disadvantage is that the mathematical labour required increases so rapidly with order that results have not been obtained beyond second order in the perturbation parameter, which effectively limits the accuracy of these results to rather small membrane deformations.

The power and attractiveness of these perturbations methods, however, has recently been enhanced substantially by the availability of symbol-manipulation computer programs like MACSYMA (Rand 1984) and REDUCE, which render tractable the monumental algebraic manipulations required to compute higher-order terms in perturbation series. We have taken advantage of one of these programs (REDUCE, Rand Corp. Santa Monica, CA) to study a simplified model of a tank-treading membrane: deformation of an initially pressurized cylindrical membrane by a slow viscous shear flow. A perturbation series through fifth order in a dimensionless shear rate parameter is easily generated by computer algebra, and when combined with a coordinate transformation yields an analytical solution which is accurate for quite large deformations of the membrane. Although this two-dimensional problem is not particularly realistic physically, our primary intent is to establish the technique of calculation – which is applicable to more realistic problems. Further, we expect that the very detailed results obtained in this analysis are at least qualitatively indicative of the behaviour of a tank-treading erythrocyte.

## 2. Mathematical formulation

Consider a thin membrane in the shape of a circular cylinder of radius $a$ and infinitely long in the axial direction. The membrane is assumed to be inextensible in a plane perpendicular to the axis of the cylinder, and is filled with an incompressible Newtonian fluid of viscosity ${}^{\mathrm{i}}\mu$†; the pressure inside the membrane is initially constant at a value of $p_0$. The membrane is surrounded by an initially stationary incompressible Newtonian fluid of viscosity ${}^{\mathrm{e}}\mu$; the exterior fluid is of unbounded extent. Let $\hat{z}$ denote distance in the direction of the axis of the cylinder and $\hat{x}$ and $\hat{y}$ denote rectangular coordinates in a plane perpendicular to the cylinder axis. If $\boldsymbol{e}_x$, $\boldsymbol{e}_y$, and $\boldsymbol{e}_z$ are unit vectors along the three coordinate axes, then the fluid velocity can be written as

$$\hat{\boldsymbol{v}} = \hat{v}_x \boldsymbol{e}_x + \hat{v}_y \boldsymbol{e}_y + \hat{v}_z \boldsymbol{e}_z. \tag{1}$$

Now suppose that a simple shear flow is generated in the external fluid which, far from the membrane, has the form

$$\hat{\boldsymbol{v}} = \dot{\gamma}\hat{y}\boldsymbol{e}_x, \tag{2}$$

† Superscripts 'i' and 'e' placed before a symbol will designate quantities appropriate to the 'interior' and 'exterior' of the membrane. A circumflex '^' will usually indicate physical, as opposed to dimensionless, quantities; exceptions are the parameters ${}^{\mathrm{e}}\mu$, ${}^{\mathrm{i}}\mu$, $p_0$, $\dot{\gamma}$, and $a$. Unit vectors are considered dimensionless.

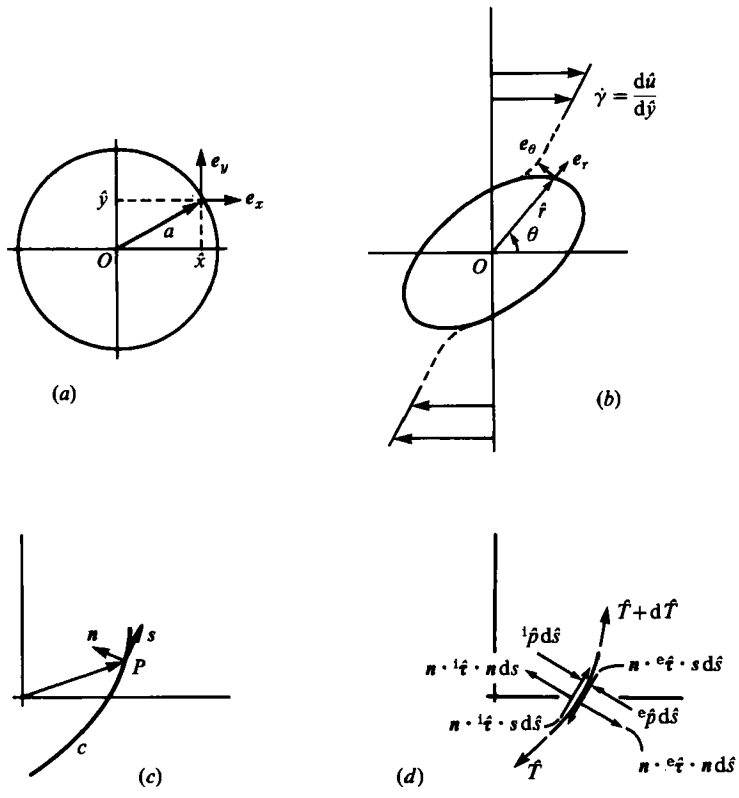


FIGURE 1. (*a*) Cross-section of the undeformed membrane. (*b*) Cross-section of the membrane deformed by a shear flow. (*c*) Tangential and normal unit vectors on the membrane. (*d*) System of forces in equilibrium which act on a membrane element.

where $\dot{\gamma}$ is a constant shear rate. We assume that this external shear flow will cause the membrane to deform and, after a starting transient, assume a stationary shape and orientation; if the origin of coordinates is on the cylinder axis, the deformed cross-section will be symmetrical about the origin. Although the steady-state shape of the membrane is assumed invariant with respect to time, the membrane will have a velocity tangent to itself; this is the motion known as 'tank treading'. This circulation of the membrane will drive an interior flow inside the membrane. The physical problem described above is illustrated schematically in figure 1. Figure 1 (*d*) shows the system of surface stresses acting on an element of the membrane. Note that $\hat{\boldsymbol{\tau}}$ represents the viscous stress tensor. We assume that the membrane is of negligible mass, and therefore the surface tractions acting on the membrane and the membrane tension, $\hat{T}$, must produce a system of forces which is in equilibrium at every point of the membrane. Further, as the membrane is assumed inextensible, its speed will be the same at every point.

Let $\hat{r}$ and $\theta$ represent polar coordinates in a plane perpendicular to the cylinder axis. Let $\hat{s}$ and $\hat{n}$ represent distances, respectively tangential and normal to the membrane, and $\boldsymbol{s}$ and $\boldsymbol{n}$ be the associated unit vectors (see figure 1). The problem can be posed in terms of a stream function $\hat{\psi}(\hat{x}, \hat{y})$ (e.g. Langlois 1964) such that

$$\hat{\boldsymbol{v}} = \hat{\boldsymbol{\nabla}} \times \hat{\psi} \boldsymbol{e}_z, \tag{3}$$

where $$\hat{\nabla} = \boldsymbol{e}_x \frac{\partial}{\partial \hat{x}} + \boldsymbol{e}_y \frac{\partial}{\partial \hat{y}} + \boldsymbol{e}_z \frac{\partial}{\partial \hat{z}}.$$

The incompressibility condition is automatically satisfied by this formulation, and the pressure $\hat{p}(\hat{x}, \hat{y})$ is given in terms of the stream function by

$$\hat{\nabla}\hat{p} = \mu \hat{\nabla} \times \hat{\nabla}^2 \psi \boldsymbol{e}_z, \tag{4}$$

where $\mu$ is the fluid viscosity.† We assume that the inertial terms in the equations of motion can be neglected, and from this it follows (Langlois 1964) that the stream function satisfies the biharmonic equation

$$\hat{\nabla}^4 \hat{\psi} = 0. \tag{5}$$

There are two important dimensionless parameters in this problem, namely

$$\epsilon = \frac{\dot{\gamma}\, {}^{\mathrm{e}}\mu}{p_0}, \tag{6}$$

the dimensionless shear rate, and

$$\beta = \frac{{}^{\mathrm{i}}\mu}{{}^{\mathrm{e}}\mu}, \tag{7}$$

the viscosity ratio.

We define the following dimensionless variables

$$(x, y, z, r, s, n) = \frac{(\hat{x}, \hat{y}, \hat{z}, \hat{r}, \hat{s}, \hat{n})}{a}, \quad \psi = \left(\frac{{}^{\mathrm{e}}\mu}{a^2 p_0}\right)\hat{\psi}, \quad p = \frac{\hat{p}}{p_0}, \quad T = \frac{\hat{T}}{a p_0}, \quad \tau = p_0^{-1}\hat{\tau}. \tag{8}$$

If $\hat{\kappa}$ is the curvature of the membrane, and $\hat{v}$ is the membrane surface speed (positive clockwise) we define

$$\left.\begin{aligned} \kappa &= a\hat{\kappa}, \quad v = \left(\frac{{}^{\mathrm{e}}\mu}{a p_0}\right)\hat{v}, \\ \text{and} \qquad \nabla &= a\hat{\nabla} = \boldsymbol{e}_x \frac{\partial}{\partial x} + \boldsymbol{e}_y \frac{\partial}{\partial y} + \boldsymbol{e}_z \frac{\partial}{\partial z}. \end{aligned}\right\} \tag{9}$$

In terms of these dimensionless variables we may formally state the problem to be solved as follows. Find a simple closed curve $C: r = f(\theta)$, interior stream function ${}^{\mathrm{i}}\psi$ and pressure ${}^{\mathrm{i}}p$, exterior stream function ${}^{\mathrm{e}}\psi$ and pressure ${}^{\mathrm{e}}p$, a membrane tension $T(\theta)$, and a surface speed $v(\epsilon, \beta)$, satisfying the following equations and boundary conditions:

$$\nabla^4 {}^{\mathrm{e}}\psi = 0, \quad \nabla {}^{\mathrm{e}}p = \nabla \times \nabla^2 {}^{\mathrm{e}}\psi \boldsymbol{e}_z \quad \text{outside } C, \tag{10}$$

$$\nabla^4 {}^{\mathrm{i}}\psi = 0, \quad \nabla {}^{\mathrm{i}}p = \beta \nabla \times \nabla^2 {}^{\mathrm{i}}\psi \boldsymbol{e}_z \quad \text{inside } C, \tag{11}$$

$${}^{\mathrm{e}}\psi \to \epsilon(\tfrac{1}{4}r^2)(1 - \cos(2\theta)), \quad {}^{\mathrm{e}}p \to 0 \quad \text{as } r \to \infty, \tag{12a, b}$$

$${}^{\mathrm{i}}\psi = 0, \quad {}^{\mathrm{e}}\psi = 0 \quad \text{on } C, \tag{13}$$

$${}^{\mathrm{i}}\psi_{,n} + v(\epsilon, \beta) = 0, \quad {}^{\mathrm{e}}\psi_{,n} + v(\epsilon, \beta) = 0 \quad \text{on } C, \tag{14}$$

$$\kappa T - ({}^{\mathrm{i}}p - {}^{\mathrm{e}}p) - \boldsymbol{n} \cdot {}^{\mathrm{e}}\boldsymbol{\tau} \cdot \boldsymbol{n} + \boldsymbol{n} \cdot {}^{\mathrm{i}}\boldsymbol{\tau} \cdot \boldsymbol{n} = 0 \quad \text{on } C, \tag{15}$$

$$\frac{\mathrm{d}T}{\mathrm{d}s} - \boldsymbol{n} \cdot {}^{\mathrm{e}}\boldsymbol{\tau} \cdot \boldsymbol{s} + \boldsymbol{n} \cdot {}^{\mathrm{i}}\boldsymbol{\tau} \cdot \boldsymbol{s} = 0 \quad \text{on } C, \tag{16}$$

$$\int_0^{2\pi} (f^2 + f'^2)^{\frac{1}{2}} \,\mathrm{d}\theta = 2\pi, \tag{17}$$

† If the superscript 'i' or 'e' is omitted in an equation, the equation applies to both interior and exterior flows.

and finally
$$^{\mathrm{i}}p \to 1 \quad \text{as } r \to 0. \tag{18}$$

We also require that $^{\mathrm{i}}\psi$ be free of singularities.

In the preceding equations, and throughout the remainder of this paper we use the comma notation for partial derivatives, that is, $\psi_{,n} = (\partial\psi/\partial n)$, etc. In (15) and (16) the surface tractions are to be regarded as functions of the stream functions via the relations (the superposed dot denotes differentiation with respect to $\theta$)

$$\boldsymbol{n}\cdot{}^{\mathrm{e}}\boldsymbol{\tau}\cdot\boldsymbol{n}\dagger = 2\left[(r^2+\dot{r}^2)^{-1}\left\{r^2\left(\frac{^{\mathrm{e}}\psi_{,\theta}}{r}\right)_{,r} + r\dot{r}\left(r\left(\frac{^{\mathrm{e}}\psi_{,r}}{r}\right)_{,r} - \frac{^{\mathrm{e}}\psi_{,\theta\theta}}{r^2}\right) + \dot{r}^2\left(\frac{^{\mathrm{e}}\psi_{,\theta}}{r^2} - \frac{^{\mathrm{e}}\psi_{,r\theta}}{r}\right)\right\}\right]_{r=f(\theta)}, \tag{19}$$

$$\boldsymbol{n}\cdot{}^{\mathrm{e}}\boldsymbol{\tau}\cdot\boldsymbol{s} = \left[(r^2+\dot{r}^2)^{-1}\left\{r^2\left(r\left(\frac{^{\mathrm{e}}\psi_{,r}}{r}\right)_{,r} - \frac{^{\mathrm{e}}\psi_{,\theta\theta}}{r^2}\right) - 4r\dot{r}\left(\frac{^{\mathrm{e}}\psi_{,\theta}}{r}\right)_{,r} + \dot{r}^2\left(\frac{^{\mathrm{e}}\psi_{,\theta\theta}}{r^2} - r\left(\frac{^{\mathrm{e}}\psi_{,r}}{r}\right)_{,r}\right)\right\}\right]_{r=f(\theta)}; \tag{20}$$

The same relations hold for the interior tractions on the membrane, $\boldsymbol{n}\cdot{}^{\mathrm{i}}\boldsymbol{\tau}\cdot\boldsymbol{n}$ and $\boldsymbol{n}\cdot{}^{\mathrm{i}}\boldsymbol{\tau}\cdot\boldsymbol{s}$, except that $^{\mathrm{e}}\psi$ is replaced by $^{\mathrm{i}}\psi$, and the right-hand sides of (19) and (20) are multiplied by $\beta$. In (15) the curvature $\kappa$ is to be considered a function of $f(\theta)$ via

$$\kappa = \frac{(f^2+2\dot{f}^2-f\ddot{f})}{(f^2+\dot{f}^2)^{\frac{3}{2}}}. \tag{21}$$

The meaning of the boundary conditions is as follows. Equation (12*a*) states that the external stream function should represent a simple shear flow far from the membrane. Equation (13) states that the membrane is a streamline. Equation (14) states that the membrane surface speed is constant, and that the fluid velocity is continuous across the membrane. Equations (15) and (16) are, respectively, the membrane equilibrium conditions in directions normal and tangential to the membrane.† The membrane inextensibility condition is expressed by (17). Finally, the conditions on the pressure are given by (12*b*), and (18). The first of these simply states that the remote pressure is the reference with respect to which pressure is measured. Equation (18) implies that the pressure at the origin is maintained at $p_0$, regardless of the degree of deformation. This last boundary condition determines uniquely the interior pressure and is made necessary by the assumed inextensibility of the membrane; further comments on this internal pressure condition will appear in §7.

Before describing the method of solution, we note that since $\psi$ satisfies the two-dimensional biharmonic equation it can be represented very compactly in terms of two analytic functions of a complex variable via the 'Goursat representation' (Muskhelishvili 1953; Langlois 1964). Thus if Re( ), Im( ), $\bar{(\ )}$, and j denote respectively the real part, imaginary part, complex conjugate, and imaginary unit, there exist two analytic functions $\chi$ and $\phi$ of a complex variable $z = x+\mathrm{j}y$ such that

$$\psi(x,y) = \mathrm{Re}\{\chi(z)+\bar{z}\phi(z)\}. \tag{22}$$

In terms of these analytic functions the velocity field is given by

$$v_x+\mathrm{j}v_y = -\mathrm{j}(\phi+z\bar{\phi}'+\bar{\chi}'), \tag{23}$$

† It can be shown that the normal viscous stress $\boldsymbol{n}\cdot\boldsymbol{\tau}\cdot\boldsymbol{n}$ vanishes in the problem treated in this paper, as a consequence of membrane inextensibility. This term, however, will be non-zero in more general problems where the membrane speed is not constant.

where the prime denotes differentiation with respect to $z$. The pressure is

$$p = \mathrm{Re}\,(4\mathrm{j}\phi' + p^*), \tag{24}$$

where $p^*$ is a complex constant, and the viscous stresses can be expressed as

$$(\tau_{yy} - \tau_{xx}) + 2\mathrm{j}\tau_{xy} = -4\mathrm{j}(\chi'' + \bar{z}\phi''). \tag{25}$$

Further, the total force, $F_x + \mathrm{j}F_y$, and moment $M$ (per unit width of flow) which the fluid exerts on a surface represented by an arbitrary curve connecting a point $A$ to a point $B$, can be calculated from

$$F_x + \mathrm{j}F_y = [2(\overline{\chi'} + z\overline{\phi'} - \phi)]_A^B, \tag{26}$$

and

$$M = \mathrm{Re}\,[2\mathrm{j}(z\bar{z}\phi' + z\chi' - \chi)]_A^B, \tag{27}$$

where $[\ ]_A^B$ represents the value of a function at point $A$ minus its value at point $B$; the force and moment are those exerted by the fluid on the right of the curve as the curve is traversed from $A$ to $B$. Equations (24) to (27) are valid as written for the exterior flow, but due to the scaling we have used in defining our dimensionless variables, the right-hand sides of these equations must be multiplied by $\beta$ for the interior flow. We will use the Goursat representation for a concise presentation of our results.

## 3. Expansion in powers of $\epsilon$

Clearly, as the dimensionless shear rate $\epsilon$ goes to zero, our problem has the trivial solution

$$^{\mathrm{e}}\psi = {}^{\mathrm{i}}\psi = {}^{\mathrm{e}}p = v = 0, \quad {}^{\mathrm{i}}p = T = f = 1.$$

For $\epsilon \neq 0$ we seek to represent the solution as a power series in $\epsilon$ as follows

$$\left.\begin{aligned} {}^{\mathrm{e}}\psi &= \sum_{n=1}^{\infty} \epsilon^n\, {}^{\mathrm{e}}\psi^{(n)}, \quad {}^{\mathrm{i}}\psi = \sum_{n=1}^{\infty} \epsilon^n\, {}^{\mathrm{i}}\psi^{(n)}, \quad {}^{\mathrm{e}}p = \sum_{n=1}^{\infty} \epsilon^n\, {}^{\mathrm{e}}p^{(n)}, \\ {}^{\mathrm{i}}p &= \sum_{n=0}^{\infty} \epsilon^n\, {}^{\mathrm{i}}p^{(n)}, \quad f = \sum_{n=0}^{\infty} \epsilon^n r_n, \quad T = \sum_{n=0}^{\infty} \epsilon^n T_n. \end{aligned}\right\} \tag{28}$$

The coefficients in these expansions depend on $r$, $\theta$, and $\beta$, except that $r_n$ and $T_n$ are independent of $r$; obviously, ${}^{\mathrm{i}}p^{(0)} = r_0 = T_0 = 1$. Consistent with the above assumptions we expand the viscous stress tensor and the surface speed as

$${}^{\mathrm{e}}\boldsymbol{\tau} = \sum_{n=1}^{\infty} \epsilon^n\, {}^{\mathrm{e}}\boldsymbol{\tau}^{(n)}, \quad {}^{\mathrm{i}}\boldsymbol{\tau} = \sum_{n=1}^{\infty} \epsilon^n\, {}^{\mathrm{i}}\boldsymbol{\tau}^{(n)}, \quad v = -\sum_{n=1}^{\infty} \epsilon^n v^{(n)}(\beta). \tag{29}$$

When these expansions are inserted into the equations and boundary conditions, (10) to (18), and the coefficients of like powers of $\epsilon$ are equated, there results a sequence of boundary-value problems, each of which can be solved uniquely by methods described below. Thus, in principle, an arbitrary number of terms of the series could be determined, but the algebraic labour increases so rapidly that hand calculations are impractical beyond $O(\epsilon^2)$. The series-expansion approach, however, overcomes the most serious difficulty of the original problem: the boundary conditions, (13) to (16), to be applied on the unknown boundary, $r = f(\theta)$, are 'transferred' by the

expansion to the fixed unit circle, $r = 1$. For any function, $F(r, \theta; \epsilon, \beta)$, to be evaluated on $r = f(\theta)$ we can combine the expansions

$$F(r,\theta) = F^{(0)}(r,\theta) + F^{(1)}(r,\theta) + F^{(2)}(r,\theta) + \ldots,$$

and

$$f(\theta) = 1 + \epsilon r_1(\theta) + \epsilon^2 r_2(\theta) + \ldots,$$

to yield

$$F(f(\theta),\theta) = F^{(0)} + \epsilon(F^{(1)} + r_1 F^{(0)}_{,r}) + \epsilon^2(F^{(2)} + r_1 F^{(1)}_{,r} + r_2 F^{(0)}_{,r} + \tfrac{1}{2} r_1^2 F^{(0)}_{,rr}) + \ldots. \quad (30)$$

The expansion of the equations and boundary conditions is a tedious but purely mechanical process. In Rao (1985) are listed the complete first-order, ($O(\epsilon)$), and second-order, ($O(\epsilon^2)$), problems. Specifically, the first-order problem is

$$\nabla^4 {}^{\mathrm{e}}\psi^{(1)} = 0, \quad \nabla^4 {}^{\mathrm{i}}\psi^{(1)} = 0, \quad (31)$$

$$\nabla {}^{\mathrm{e}}p^{(1)} = \nabla \times \nabla^2 {}^{\mathrm{e}}\psi^{(1)} \boldsymbol{e}_z, \quad \nabla {}^{\mathrm{i}}p^{(1)} = \beta \nabla \times \nabla^2 {}^{\mathrm{i}}\psi^{(1)} \boldsymbol{e}_z. \quad (32)$$

As $r \to \infty$,

$${}^{\mathrm{e}}\psi^{(1)} \to (\tfrac{1}{4} r^2)(1 - \cos(2\theta)), \quad {}^{\mathrm{e}}p^{(1)} \to 0. \quad (33a, b)$$

On $r = 1$,

$${}^{\mathrm{e}}\psi^{(1)} = {}^{\mathrm{i}}\psi^{(1)} = 0, \quad (34)$$

$${}^{\mathrm{e}}\psi^{(1)}_{,r} = {}^{\mathrm{i}}\psi^{(1)}_{,r} = v_1(\beta), \quad (35)$$

$$T_1 - (\ddot{r}_1 + r_1) = ({}^{\mathrm{i}}p^{(1)} - {}^{\mathrm{e}}p^{(1)}) - 2({}^{\mathrm{e}}\psi^{(1)}_{,\theta} - {}^{\mathrm{e}}\psi^{(1)}_{,r\theta}) + 2\beta({}^{\mathrm{i}}\psi^{(1)}_{,\theta} - {}^{\mathrm{i}}\psi^{(1)}_{,r\theta}), \quad (36)$$

$$T_1^{\dagger} = -({}^{\mathrm{e}}\psi^{(1)}_{,r} - {}^{\mathrm{e}}\psi^{(1)}_{,rr} + {}^{\mathrm{e}}\psi^{(1)}_{,\theta\theta}) + \beta({}^{\mathrm{i}}\psi^{(1)}_{,r} - {}^{\mathrm{i}}\psi^{(1)}_{,rr} + {}^{\mathrm{i}}\psi^{(1)}_{,\theta\theta}). \quad (37)$$

Also

$$\int_0^{2\pi} r_1 \, \mathrm{d}\theta = 0, \quad (38)$$

and

$${}^{\mathrm{i}}p^{(1)} \to 0 \quad \text{as } r \to 0. \quad (39)$$

A procedure for solving this first-order problem will be described in detail; exactly the same procedure was employed to solve the higher-order problems. First we note that (22) implies that both the interior and exterior stream functions can be written in the form

$$\psi^{(1)} = \psi_1^{(1)} + (r^2 - 1)\psi_2^{(1)}, \quad (40)$$

where $\psi_1^{(1)}$ and $\psi_2^{(1)}$ are harmonic functions. As $\psi^{(1)}$ must be periodic in $\theta$ with period $2\pi$ we can expand in terms of cylindrical harmonics (Duff & Naylor 1966)

$$\psi_1^{(1)} = A_0 + B_0 \log(r) + \sum_{n=1}^{\infty} (A_n r^n + C_n r^{-n}) \cos(n\theta) + (B_n r^n + D_n r^{-n}) \sin(n\theta), \quad (41)$$

with a similar expression for $\psi_2^{(1)}$. This in turn, implies that each of the analytic functions $\chi_1(z)$ and $\phi_1(z)$ is of the form†

$$C_0 \log(z) + \sum_{n=-\infty}^{\infty} C_n z^n. \quad (42)$$

In order that the interior stream function have no singularities the logarithmic term and all negative powers of $z$ must be absent from the interior expansion. Thus the most general acceptable form of the interior first-order stream function is

$${}^{\mathrm{i}}\psi^{(1)} = \sum_{n=0}^{\infty} r^n \{{}^{\mathrm{i}}A_n \cos(n\theta) + {}^{\mathrm{i}}B_n \sin(n\theta)\} + (r^2 - 1) \sum_{n=0}^{\infty} r^n \{{}^{\mathrm{i}}C_n \cos(n\theta) + {}^{\mathrm{i}}D_n \sin(n\theta)\}. \quad (43)$$

† The notation here is $\psi^{(m)} = \mathrm{Re}\{\chi_m(z) + \bar{z}\phi_m(z)\}$.

Turning to the exterior stream function, it can be seen from (33) that ${}^{e}\phi_1 = O(z)$ and ${}^{e}\chi_1 = O(z^2)$ as $z \to \infty$. Further it can be shown (Rao 1985), as a consequence of (26) and (27) and the requirement that the resultant force and moment exerted by the exterior flow on the membrane be zero, that the logarithmic term is absent from both ${}^{e}\chi_1$ and ${}^{e}\phi_1$. Thus the most general acceptable form for the exterior first-order stream function is

$$ {}^{e}\psi^{(1)} = r^2\{{}^{e}A_{-2}\cos(2\theta) + {}^{e}B_{-2}\sin(2\theta)\} + \sum_{n=-1}^{\infty} r^{-n}\{{}^{e}A_n\cos(n\theta) + {}^{e}B_n\sin(n\theta)\} + (r^2-1)\sum_{n=0}^{\infty} r^{-n}\{{}^{e}C_n\cos(n\theta) + {}^{e}D_n\sin(n\theta)\}. \quad (44) $$

Similar reasoning shows that (43) and (44) are also the most general acceptable forms for the higher-order exterior and interior stream functions, if the first term in braces on the right-hand side of (44) is deleted. Starting with (33) and (34), the complete solution to the first-order problem can be easily constructed by evaluating the coefficients in the trigonometric series via the boundary conditions.

Step 1: Using (43) in conjunction with (34) gives

$$ {}^{i}A_n = {}^{i}B_n = 0 \text{ for all } n. $$

Step 2: Imposing (35) gives ${}^{i}C_0 = \frac{1}{2}v^{(1)}$, and all the other

$${}^{i}C_n \text{ and } {}^{i}D_n \text{ are zero.}$$

Step 3: Using (44) in conjunction with (33) gives ${}^{e}C_0 = \frac{1}{4}$ and

$$ {}^{e}A_{-2} = -\tfrac{1}{4} \text{ and } {}^{e}B_{-2} = 0. $$

Step 4: Imposing (34) gives ${}^{e}A_2 = \frac{1}{4}$, and all the other

$${}^{e}A_n \text{ and } {}^{e}B_n \text{ equal to zero.}$$

Step 5: Imposing (35) gives ${}^{e}C_2 = \frac{1}{2}$ and $v^{(1)} = \frac{1}{2}$ (this is the step which determines the surface speed). At this point the first-order stream function has been uniquely determined as

$$ {}^{i}\psi^{(1)} = (\tfrac{1}{4})(r^2-1), \quad (45) $$

and

$$ {}^{e}\psi^{(1)} = \tfrac{1}{4}[(r^2-1) + \cos(2\theta)(2-r^{-2}-r^2)]. \quad (46) $$

Step 6: Next the interior and exterior pressure fields, ${}^{i}p^{(1)}$ and ${}^{e}p^{(1)}$, are determined by integrating (32), subject to the boundary conditions imposed by (33$b$) and (39). Thus the first-order pressure fields are uniquely determined as

$$ {}^{i}p^{(1)} = 0, \quad {}^{e}p^{(1)} = -2r^{-2}\sin(2\theta). \quad (47) $$

Step 7: The first-order membrane tension, $T_1(\theta)$ is determined by integrating (37), which yields

$$ T_1(\theta) = C_T^{(1)} - \sin(2\theta), \quad (48) $$

where $C_T^{(1)}$ is a constant of integration.

Step 8: The first-order shape change of the membrane is determined by integrating (36) for $r_1(\theta)$. In this integration the homogeneous solution is discarded as it represents a rigid-body translation of membrane, leaving

$$ r_1(\theta) = C_T^{(1)} + \sin(2\theta). \quad (49) $$

Step 9: Finally, the constant of integration is determined by the inextensibility condition, (equation (38)), as $C_T^{(1)} = 0$.

At this point the complete first-order solution $({}^e\psi^{(1)}, {}^i\psi^{(1)}, {}^ep^{(1)}, {}^ip^{(1)}, T_1, r_1, v^{(1)})$ has been determined uniquely.

The forms of the higher-order problems are similar to the form of the first-order problem as expressed by (31) to (39). Thus (31), (32), (39), and (33*b*) hold for all higher-order problems. Equation (33*a*) is replaced by ${}^e\psi^{(n)} = o(r^2)$ as $r \to \infty$, whereas the right-hand sides of (34) to (37), and the integrand of (38), depend for each order on the solutions of the lower-order problems. Given that for each order the interior and exterior stream functions can be represented by trigonometric series of the form of (43) and (44), the procedure outlined in Steps 1 to 9 above was followed to construct uniquely the solutions to the higher-order problems. Although the solution procedure is, in principle, straightforward and simple, as in all perturbation analyses of this type the size of the problems and the algebraic workload grows rapidly with order.

Therefore the problem was programmed on a VAX 11/750 computer employing the algebraic symbol-manipulation program REDUCE. This program had the capabilities to execute, in symbolic terms, all the operations needed not only to solve the higher-order problems but also to formulate them; these operations included series expansion, and differentiation and integration of polynomials and trigonometric functions. Due to space limitations we must forego an account of the programming details here; these details, together with listings of the programs actually used, are available in Rao (1985).

## 4. The solution, up to $O(\epsilon^5)$

The series solution to the problem described in the preceding sections was constructed up to $O(\epsilon^5)$. This solution can be expressed compactly in the Goursat representation as follows

$$\psi(x, y) = \mathrm{Re}\left\{ \sum_{m=1}^{\infty} \epsilon^m \chi_m + \bar{z} \sum_{m=1}^{\infty} \epsilon^m \phi_m \right\}, \tag{50}$$

where

$$\chi_m(z) = \sum_n A_{mn}(\beta)\, z^n, \quad \phi_m(z) = \sum_n B_{mn}(\beta)\, z^n. \tag{51}$$

These forms apply to both the external and internal stream functions, and the coefficients $A_{mn}$ and $B_{mn}$ for $m = 1$ to 5 are listed in tables 1 and 2 (external and internal, respectively). In addition to the stream function, (50), the solution algorithm simultaneously yielded series for the pressure, viscous stress, membrane tension, membrane shape, and surface speed; these expansions will not be listed separately as, in principle, they can all be derived from (50). Thus, for example, the pressure can be computed directly via (34), and the membrane shape expansion

$$r = 1 + \sum_{n=1}^{\infty} r_n(\theta)\, \epsilon^n$$

can be obtained, through $O(\epsilon^5)$, from the condition $\psi = 0$ on the membrane, using either the external or internal stream function. For reference in further discussion, however, we note the following two points. To $O(\epsilon^2)$ the membrane shape is given by

$$r = 1 + \epsilon \sin(2\theta) - \epsilon^2\{1 - (1+\beta)\cos(2\theta) + \tfrac{3}{4}\cos(4\theta)\} + \ldots; \tag{52}$$

| | $m$ | 1 | 2 | 3 | 4 | 5 |
|---|---|---|---|---|---|---|
| | $n$ | | | | | |
| | 2 | $-\frac{1}{4}$ | 0 | 0 | 0 | 0 |
| | 0 | $-\frac{1}{4}$ | 0 | $\frac{5}{8}$ | 0 | $-\frac{5}{6}\beta^2-\frac{7}{4}\beta-\frac{121}{128}$ |
| | $-2$ | $-\frac{1}{4}$ | $\frac{1}{4}$j | $\frac{1}{4}(\beta+1)$ | j$(-\frac{1}{4}\beta^2-\frac{1}{2}\beta+\frac{1}{32})$ | $-\frac{1}{4}\beta^3-\frac{5}{4}\beta^2-\frac{31}{32}\beta+\frac{9}{64}$ |
| $A_{mn}$ | $-4$ | 0 | $-\frac{1}{2}$j | $-\frac{1}{16}(8\beta+17)$ | j$(\frac{1}{2}\beta^2+\frac{17}{8}\beta+\frac{15}{8})$ | $\frac{1}{2}\beta^3+\frac{67}{16}\beta^2+\frac{25}{4}\beta+\frac{35}{16}$ |
| | $-6$ | 0 | 0 | $\frac{5}{4}$ | j$(-\frac{5}{2}\beta-\frac{129}{32})$ | $-\frac{15}{4}\beta^2-\frac{387}{32}\beta-\frac{307}{32}$ |
| | $-8$ | 0 | 0 | 0 | $\frac{7}{2}$j | $\frac{21}{2}\beta+\frac{3861}{256}$ |
| | $-10$ | 0 | 0 | 0 | 0 | $-\frac{21}{2}$ |
| | 1 | $\frac{1}{4}$ | 0 | 0 | 0 | 0 |
| | $-1$ | $\frac{1}{2}$ | $-\frac{3}{4}$j | $-\frac{1}{4}(3\beta+4)$ | j$(\frac{3}{4}\beta^2+2\beta+\frac{37}{32})$ | $\frac{3}{4}\beta^3+\frac{9}{2}\beta^2+\frac{165}{32}\beta+\frac{95}{64}$ |
| $B_{mn}$ | $-3$ | 0 | $\frac{1}{2}$j | $\frac{1}{16}(8\beta+21)$ | j$(-\frac{1}{2}\beta^2-\frac{21}{8}\beta-\frac{21}{8})$ | $-\frac{1}{2}\beta^3-\frac{79}{16}\beta^2-\frac{17}{2}\beta-\frac{137}{32}$ |
| | $-5$ | 0 | 0 | $-1$ | j$(2\beta+\frac{119}{32})$ | $3\beta^2+\frac{357}{32}\beta+\frac{309}{32}$ |
| | $-7$ | 0 | 0 | 0 | $-\frac{5}{2}$j | $-\frac{15}{2}\beta-\frac{3069}{256}$ |
| | $-9$ | 0 | 0 | 0 | 0 | 7 |

Note: All coefficients other than those listed, in the polynomials defining ${}^{e}\chi_m$ and ${}^{e}\phi_m$, are zero.

TABLE 1. Coefficients in the expansion of the external complex stream function

$${}^{e}\chi_m(z)=\sum_n A_{mn}(\beta)\,z^n \quad \text{and} \quad {}^{e}\phi_m(z)=\sum_n B_{mn}(\beta)\,z^n$$

| | $m$ | 1 | 2 | 3 | 4 | 5 |
|---|---|---|---|---|---|---|
| | $n$ | | | | | |
| | 0 | $-\frac{1}{4}$ | 0 | $\frac{1}{8}(4\beta+9)$ | 0 | $-\frac{1}{2}\beta^3-\frac{25}{8}\beta^2-\frac{11}{2}\beta-\frac{681}{128}$ |
| | 2 | 0 | $\frac{3}{4}$j | $-\frac{13}{4}(\beta+1)$ | j$(-\frac{3}{4}\beta^2-3\beta-\frac{117}{32})$ | $\frac{3}{4}\beta^3+\frac{21}{4}\beta^2+\frac{261}{32}\beta+\frac{117}{32}$ |
| $A_{mn}$ | 4 | 0 | 0 | $\frac{7}{16}$ | j$(\frac{7}{8}\beta+\frac{7}{8})$ | $-\frac{21}{16}\beta^2-\frac{7}{2}\beta-\frac{63}{16}$ |
| | 6 | 0 | 0 | 0 | $-\frac{11}{32}$j | $\frac{33}{32}\beta+\frac{33}{32}$ |
| | 8 | 0 | 0 | 0 | 0 | $-\frac{75}{256}$ |
| | 1 | $\frac{1}{4}$ | 0 | $-\frac{1}{2}(\beta+1)$ | 0 | $\frac{1}{2}\beta^3+\frac{5}{2}\beta^2+3\beta+\frac{35}{8}$ |
| | 3 | 0 | $-\frac{1}{4}$j | $\frac{1}{4}(\beta+1)$ | j$(\frac{1}{4}\beta^2+\beta+\frac{63}{32})$ | $-\frac{1}{4}\beta^3-\frac{7}{4}\beta^2-\frac{111}{32}\beta-\frac{63}{32}$ |
| $B_{mn}$ | 5 | 0 | 0 | $-\frac{3}{16}$ | j$(-\frac{3}{8}\beta-\frac{3}{8})$ | $\frac{9}{16}\beta^2+\frac{3}{2}\beta+\frac{51}{32}$ |
| | 7 | 0 | 0 | 0 | $\frac{5}{32}$j | $-\frac{15}{32}\beta-\frac{15}{32}$ |
| | 9 | 0 | 0 | 0 | 0 | $\frac{35}{256}$ |

Note: All coefficients other than those listed, in the polynomials ${}^{i}\chi_m$ and ${}^{i}\phi_m$, are zero.

TABLE 2. Coefficients in the expansion of the internal complex stream function

$${}^{i}\chi_m(z)=\sum_n A_{mn}(\beta)\,z^n \quad \text{and} \quad {}^{i}\phi_m(z)=\sum_n B_{mn}(\beta)\,z^n$$

for small $\epsilon$ this is approximately an ellipse with its major axis inclined to the horizontal direction by an angle

$$\theta_0=\tfrac{1}{4}\pi-\tfrac{1}{2}\epsilon(1+\beta)+\ldots. \tag{53}$$

To $O(\epsilon^5)$ the surface speed is

$$v=\tfrac{1}{2}\epsilon-(\beta+\tfrac{1}{4})\,\epsilon^3+\{\beta^3+\tfrac{17}{4}\beta^2+3\beta+\tfrac{17}{64}\}\,\epsilon^5+\ldots. \tag{54}$$

Note that the surface speed was found to be an odd function of $\epsilon$, as it must be on physical grounds.

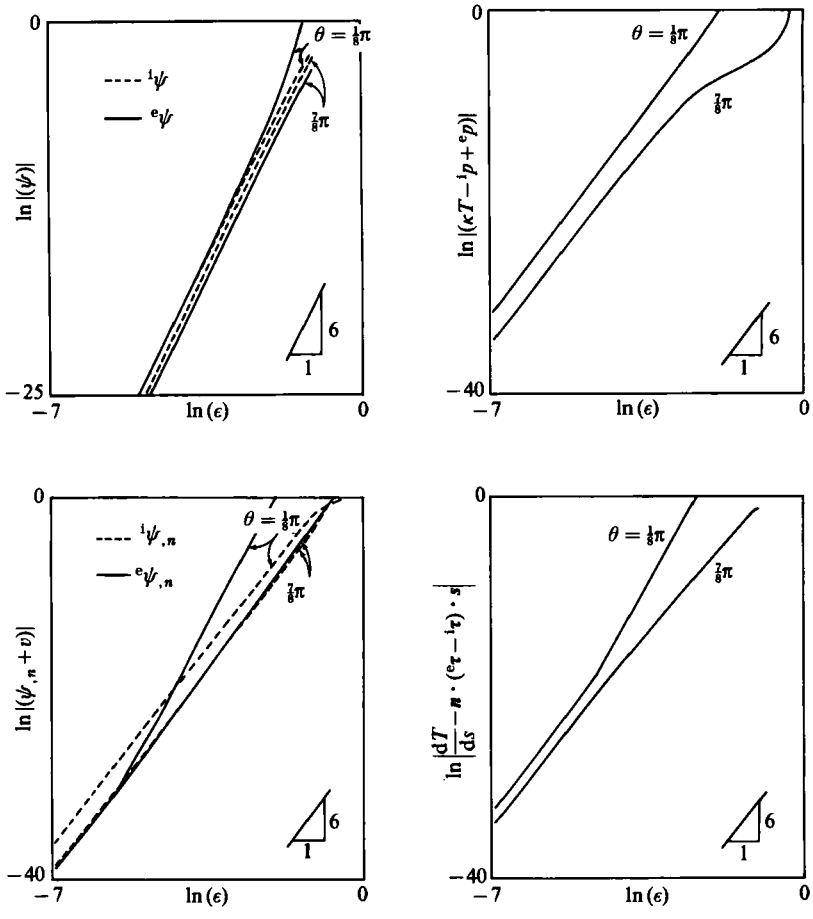


FIGURE 2. Magnitudes of the left-hand sides of the boundary conditions, (13), (14), (15) and (16) as a function of $\epsilon$ at two positions $\theta = \frac{1}{8}\pi$ and $\theta = \frac{7}{8}\pi$ on the membrane, with $\beta = 2$. The ordinates were computed by inserting into the left-hand sides of the boundary conditions the truncated $O(\epsilon^5)$ (untransformed) expansion for each variable appearing in the boundary conditions and evaluating the required expressions with $r(\theta; \epsilon, \beta)$ given by the $O(\epsilon^5)$ expansion of the membrane shape. Note that with log–log scales each curve approaches a straight line with a slope of 6 as $\epsilon \to 0$, verifying that the boundary conditions are satisfied through $O(\epsilon^5)$.

One serious problem with computer-algebra solutions which produce large series expansions is that of verification: How is one to have confidence that the solution does indeed satisfy the boundary conditions to the stated order? (The governing differential equations are obviously satisfied by a solution of the given form.) We have accomplished this verification numerically. The right-hand sides of (13) to (17) were computed, using the truncated $O(\epsilon^5)$ expansions of all the field variables which had been obtained as the solution, and the logarithms of the absolute values of these right-sides were plotted – for two values of $\theta$ – versus $\ln(\epsilon)$, as in figure 2. It can be seen that as $\epsilon$ approaches zero each of the curves in figure 2 approaches a straight line with a slope of 6. This shows that if the $O(\epsilon^5)$ solution we have constructed is inserted into the boundary conditions, then the values of the boundary operators differ from the required value of zero by quantities of $O(\epsilon^6)$ – confirming that our

solution satisfies the boundary conditions through $O(\epsilon^5)$. On this basis one can have confidence that (50) together with the coefficients listed in tables 1 and 2 is the unique expansion of the exact solution to this problem through fifth order in $\epsilon$.

Rao (1985) has undertaken a careful examination of the accuracy of this solution. Without going into details, some of which will be repeated later in this paper, it can be stated that he concluded that (i) all field variables – membrane shape, tension, viscous stresses, pressure, and velocities – were accurate for membrane deformations up to an aspect ratio, $(r_{\max}/r_{\min})$, of about 1.5, and (ii) the membrane shape and streamlines were accurate up to an aspect ratio of about 1.8. This is an improvement on an expansion truncated at $O(\epsilon^2)$ (like that of Barthes-Biesel 1980)) which is only accurate in the membrane shape up to an aspect ratio of 1.5 – and correspondingly less for velocities and stresses. This rather modest improvement in accuracy of the $O(\epsilon^5)$ expansion versus the $O(\epsilon^2)$ expansion is somewhat disappointing and can be traced to a probably limited range of convergence of the expansion of the membrane shape function in powers of $\epsilon$. As an analogy, it can be easily shown (Rao 1985) that the expansion of an ellipse $r = \{(\cos^2(\theta)/a^2) + (\sin^2(\theta)/b^2)\}^{-\frac{1}{2}}$, subject to the (approximate) constraint of constant length $a^2 + b^2 =$ constant, in powers of the eccentricity will diverge when the aspect ratio $(a/b)$ exceeds $\sqrt{3} = 1.732\ldots$ which is close to the accuracy-limiting value of 1.8 found by Rao.

The range of accuracy of our solution can be extended considerably, however, by introducing a conformal mapping from the physical plane $z = x + \mathrm{j}y$ to an auxiliary plane $\zeta = \xi + \mathrm{j}\eta$. This does not require re-solving the problem, and can be accomplished with little additional work. We will introduce this expansion and examine the accuracy of the transformed solution in the next section, before proceeding to a presentation of detailed results.

## 5. A conformal transformation

As $\epsilon$ approaches zero the deformed membrane shape approaches an ellipse; the major axis of this ellipse starts at an inclination of 45° to the horizontal (i.e. the shear direction) when $\epsilon \to 0$ and rotates towards the horizontal as $\epsilon$ increases. Thus although the problem is formulated and solved most easily in cylindrical polar coordinates, a more 'natural' coordinate system for this problem is one where one family of coordinate curves are inclined ellipses. It was expected – and was subsequently confirmed – that the introduction of such a coordinate transformation would improve the range of validity of our solution. A *conformal* transformation was chosen because this retains the simplicity of the Goursat representation for the calculation of velocities and stresses. To map the region outside and including the membrane we have used the simple Joukowski transformation

$$z = \mathrm{e}^{\mathrm{j}\theta^*}\left(\zeta + \frac{\epsilon}{\zeta}\right), \tag{55}$$

where

$$\theta^*(\epsilon, \beta) = (\tfrac{1}{4}\pi) - \tfrac{1}{2}\epsilon(1+\beta),$$

(see (53)). Thus as $\epsilon$ approaches zero the membrane is mapped onto the unit circle in the $\zeta$-plane. This transformation maps the $\zeta$-plane outside the circle $|\zeta| = \epsilon^{\frac{1}{2}}$ onto the entire $z$-plane with a branch cut running from $z = -2\epsilon^{\frac{1}{2}}e^{\mathrm{j}\theta^*}$ to $z = 2\epsilon^{\frac{1}{2}}e^{\mathrm{j}\theta^*}$; as the mapping has singularities inside the membrane it is inappropriate for transforming the interior flow. There is indeed, as there must be by the Riemann mapping theorem, a conformal transformation which maps the interior of the unit circle in the

| | $m$ | 1 | 2 | 3 | 4 | 5 |
|---|---|---|---|---|---|---|
| | $n$ | | | | | |
| | 2 | $-\frac{1}{4}\mathrm{j}$ | $-\frac{1}{4}(\beta+1)$ | $\mathrm{j}(\frac{1}{8}\beta^2+\frac{1}{4}\beta+\frac{1}{8})$ | $(\frac{1}{24}\beta^3+\frac{1}{8}\beta^2+\frac{1}{8}\beta+\frac{1}{24})$ | $\mathrm{j}(-\frac{1}{96}\beta^4-\frac{1}{24}\beta^3-\frac{1}{16}\beta^2-\frac{1}{24}\beta-\frac{1}{96})$ |
| | 0 | $-\frac{1}{4}$ | $-\frac{1}{2}\mathrm{j}$ | $(-\frac{1}{2}\beta+\frac{1}{8})$ | $\mathrm{j}(\frac{1}{4}\beta^2+\frac{1}{2}\beta+\frac{1}{4})$ | $(\frac{1}{12}\beta^3-\frac{3}{8}\beta^2-\frac{3}{2}\beta-\frac{321}{384})$ |
| $\hat{A}_{mn}$ | $-2$ | $\frac{1}{4}\mathrm{j}$ | $-\frac{1}{4}\beta$ | $\mathrm{j}(-\frac{1}{8}\beta^3-\frac{1}{4}\beta-\frac{3}{8})$ | $(\frac{1}{24}\beta^3-\frac{3}{8}\beta-\frac{5}{96})$ | $\mathrm{j}(\frac{1}{96}\beta^4+\frac{1}{24}\beta^3+\frac{15}{16}\beta^2+\frac{25}{24}\beta+\frac{7}{64})$ |
| | $-4$ | 0 | 0 | $\frac{1}{16}$ | $\mathrm{j}(-\frac{1}{4}\beta^2-\frac{1}{2}\beta-\frac{1}{2})$ | $(\frac{1}{12}\beta^3-\frac{17}{16}\beta^2-\frac{5}{4}\beta-\frac{7}{24})$ |
| | $-6$ | 0 | 0 | 0 | $\frac{1}{32}$ | $\mathrm{j}(-\frac{1}{6}\beta^2-\frac{1}{2}\beta-\frac{1}{2})$ |
| | $-8$ | 0 | 0 | 0 | 0 | $\frac{5}{256}$ |
| | 1 | $\frac{1}{4}\mathrm{j}$ | $\frac{1}{4}(\beta+1)$ | $\mathrm{j}(-\frac{1}{32}\beta^2-\frac{1}{16}\beta-\frac{1}{32}$ | $(-\frac{1}{192}\beta^3-\frac{1}{64}\beta^3-\frac{1}{64}\beta-\frac{1}{192})$ | $\mathrm{j}(\frac{1}{1536}\beta^4+\frac{1}{384}\beta^3+\frac{1}{256}\beta^2+\frac{1}{384}\beta+\frac{1}{1536})$ |
| | $-1$ | $\frac{1}{2}$ | $\mathrm{j}\frac{1}{4}(\beta-1)$ | $(-\frac{1}{16}\beta^2-\frac{3}{8}\beta-\frac{9}{16})$ | $\mathrm{j}(-\frac{1}{96}\beta^3+\frac{13}{32}\beta^2+\frac{39}{32}\beta+\frac{17}{24})$ | $(\frac{1}{768}\beta^4+\frac{29}{64}\beta^3+\frac{433}{128}\beta^2+\frac{371}{96}\beta+\frac{259}{256})$ |
| $e^{j\pi/4}\hat{B}_{mn}$ | $-3$ | 0 | 0 | $-\frac{1}{16}\mathrm{j}$ | $(-\frac{1}{4}\beta^2-\frac{17}{32}\beta-\frac{17}{32})$ | $\mathrm{j}(\frac{1}{24}\beta^3+\frac{201}{128}\beta^2+\frac{129}{64}\beta+\frac{207}{384})$ |
| | $-5$ | 0 | 0 | 0 | $-\frac{1}{32}\mathrm{j}$ | $(-\frac{1}{4}\beta^2-\frac{23}{64}\beta-\frac{33}{64})$ |
| | $-7$ | 0 | 0 | 0 | 0 | $-\mathrm{j}(\frac{5}{256})$ |

Note: All coefficients other than those listed, in the polynomials defining ${}^{e}\hat{\chi}_m$ and ${}^{e}\hat{\phi}_m$, are zero.

TABLE 3. Coefficients in the conformally transformed expansion of the external complex stream function

$$ {}^{e}\hat{\chi}_m(\zeta) = \sum_n \hat{A}_{mn}(\beta)\,\zeta^n \quad \text{and} \quad {}^{e}\hat{\phi}_m(\zeta) = \sum_n \hat{B}_{mn}(\beta)\,\zeta^n $$

$\zeta$-plane onto the interior of an ellipse in the $z$-plane without singularities, but this transformation is so complicated (Kober 1957) that it was not considered worth transforming the interior flow – particularly as almost all quantities of interest can be calculated by an application of the simple Joukowski transformation, equation (55), to the exterior flow.

If the transformation equation (55) is inserted into (51), and the latter are expanded in powers of $\epsilon$ and truncated at $O(\epsilon^5)$ one obtains the unique expansion of the solution outside and on the membrane in terms of the transformed variable $\zeta = \xi + \mathrm{j}\eta = \rho e^{\mathrm{j}\alpha}$ and the parameters $\epsilon$ and $\beta$. Thus

$$ {}^{\mathrm{e}}\hat{\chi}_m(\zeta) = \sum_n \hat{A}_{mn}(\beta)\,\zeta^n, \quad {}^{\mathrm{e}}\hat{\phi}_m(\zeta) = \sum_n \hat{B}_{mn}(\beta)\,\zeta^n, \tag{56} $$

where the coefficients $\hat{A}_{mn}$ and $\hat{B}_{mn}$ are listed for $m = 1$ to 5 in table 3. All variables of interest can be computed from (56) via the Goursat representation, keeping in mind that the physical independent variables ($x, y$ or $r, \theta$) are related to the transformed variables ($\xi, \eta$ or $\rho, \alpha$) via (55). For example, the exterior stream function is given by

$$ {}^{\mathrm{e}}\psi(\zeta) = \mathrm{Re}\left\{ \sum_{m=1}^{\infty} \epsilon^m \hat{\chi}_m + \left(\bar{\zeta} + \frac{\epsilon}{\bar{\zeta}}\right) \sum_{m=1}^{\infty} \epsilon^m \hat{\phi}_m \right\}, \tag{57} $$

and the external pressure is given by

$$ {}^{\mathrm{e}}p(\zeta) = \mathrm{Re}\left\{ 4j \left(\frac{\mathrm{d}z}{\mathrm{d}\zeta}\right)^{-1} \sum_{m=1}^{\infty} \epsilon^m \frac{\mathrm{d}\hat{\phi}_m}{\mathrm{d}\zeta} + p^* \right\}. \tag{58} $$

The above expressions for ${}^{\mathrm{e}}\psi$ and ${}^{\mathrm{e}}p$, as well as the corresponding expressions for all other variables, must be expanded in powers of $\epsilon$ and truncated at $O(\epsilon^5)$ before computation, in order to maintain consistency with the $O(\epsilon^5)$ accuracy of the original solution, (50) and (51). In the $\zeta$-plane the image of the membrane, ${}^{\mathrm{e}}\psi = 0$ is given by

$$ \begin{aligned} \rho(\alpha;\epsilon,\beta) = {} & 1 - \tfrac{1}{4}\epsilon^2 - \epsilon^3\{\tfrac{1}{2}\beta^2 + \beta + 1\}\cos(2\alpha) \\ & + \epsilon^4\{(\tfrac{1}{4}\beta^2 + \tfrac{1}{2}\beta + \tfrac{19}{64}) + (\tfrac{1}{3}\beta^3 + 3\beta^2 + 3\beta + \tfrac{1}{3})\sin(2\alpha) \\ & - (\tfrac{1}{2}\beta^2 + \beta + 1)\cos(4\alpha)\} + \epsilon^5\{(\tfrac{1}{3}\beta^3 + 3\beta^2 + 2\beta + \tfrac{1}{3})\sin(4\alpha) \\ & + (\tfrac{3}{8}\beta^4 + \tfrac{7}{2}\beta^3 + \tfrac{55}{8}\beta^2 + \tfrac{19}{4}\beta + \tfrac{33}{32})\cos(2\alpha) \\ & - (\tfrac{1}{2}\beta^2 + \beta + 1)\cos(6\alpha)\} + \ldots . \end{aligned} \tag{59} $$

Also, the membrane tension in transformed coordinates is

$$ \begin{aligned} T(\alpha;\epsilon,\beta) = {} & 1 - \epsilon\cos(2\alpha) - \epsilon^2\{(\beta+1)\sin(2\alpha) + \tfrac{1}{4}\cos(4\alpha)\} \\ & - \epsilon^3\{\tfrac{1}{4}(\beta+1)\sin(4\alpha) - (\tfrac{1}{2}\beta^2 + \beta + \tfrac{7}{8})\cos(2\alpha) + \tfrac{1}{8}\cos(6\alpha)\} \\ & - \epsilon^4\{(\tfrac{1}{2}\beta^2 + \beta + 1) - (\tfrac{1}{6}\beta^3 + \tfrac{1}{2}\beta^2 + \tfrac{53}{8}\beta + \tfrac{7}{24})\sin(2\alpha) \\ & + \tfrac{1}{8}(\beta+1)\sin(6\alpha) - (\tfrac{3}{4}\beta^2 + \tfrac{3}{2}\beta + \tfrac{11}{8})\cos(4\alpha) \\ & + \tfrac{5}{64}\cos(8\alpha)\} + \epsilon^5\{(\tfrac{1}{4}\beta^3 - \tfrac{7}{4}\beta^2 - \tfrac{5}{4}\beta + \tfrac{3}{4})\sin(4\alpha) \\ & - \tfrac{5}{64}(\beta+1)\sin(8\alpha) - (\tfrac{1}{24}\beta^4 + \tfrac{1}{6}\beta^3 \\ & + \tfrac{25}{16}\beta^2 + \tfrac{67}{24}\beta + \tfrac{13}{6})\cos(2\alpha) \\ & + (\tfrac{15}{16}\beta^2 + \tfrac{15}{8}\beta + \tfrac{225}{128})\cos(6\alpha) \\ & - \tfrac{7}{128}\cos(10\alpha)\} + \ldots . \end{aligned} \tag{60} $$

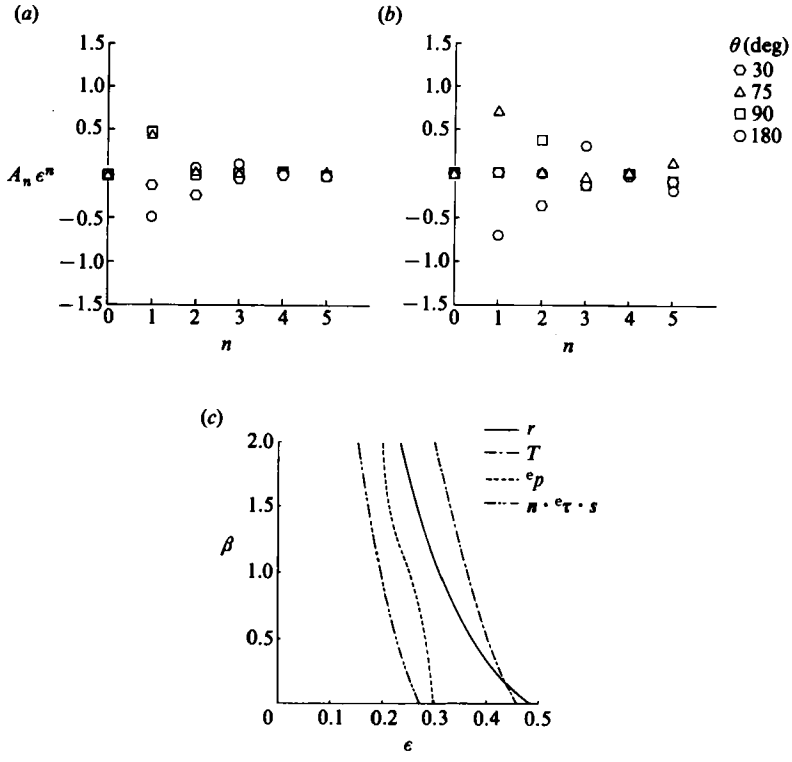


FIGURE 3. Convergence and accuracy of the conformally transformed expansions. (*a*) Successive terms in the expansion of the external shear stress,

$$\boldsymbol{n}\cdot{}^{e}\boldsymbol{\tau}\cdot\boldsymbol{s} = \sum_{n=0}^{5} A_n \epsilon^n,$$

on the membrane at four positions, with $\epsilon = 0.25$ and $\beta = 0.5$. Note the rapid decrease in the magnitude of successive terms indicating convergence. (*b*) Same as (*a*) except that $\epsilon = 0.35$. Note the slow decrease of successive terms indicating marginal convergence or divergence. (*c*) Accuracy limits of the conformally-transformed $O(\epsilon^5)$ expansions for four variables. Each curve shows the maximum value that $\epsilon$ can assume for a given $\beta$ in order that the absolute value of the last (i.e. $O(\epsilon^5)$) contribution to the variable be everywhere less than 5% of the 'characteristic magnitude' of that variable. The 'characteristic magnitude' measures the typical values of a variable and was chosen as the maximum absolute value that the variable assumes on the membrane at a given $\epsilon$ and $\beta$, as computed from the $O(\epsilon^5)$ expansion.

An examination of the accuracy of the transformed solution reveals the improvement achieved by the conformal mapping. Figure 3(*a*, *b*) illustrates for one variable, the external shear stress on the membrane, how the magnitudes of the successive terms in the series vary with the order, $n$, at several values of the polar angle $\theta$, with $\beta = 0.5$. For $\epsilon = 0.25$ (figure 3*a*) the terms decrease rapidly and the series clearly converges for all $\theta$, but when $\epsilon$ is increased to 0.35 the terms decrease slowly, at least for certain values of $\theta$, and the series begins to show signs of divergence. As an arbitrary but practical limit of accuracy we have computed the maximum value of $\epsilon$ for which the $O(\epsilon^5)$ term in the series for a given variable contributes no more to the value of the variable than 5% of the 'characteristic magnitude' of that variable. The results are presented in figure 3(*c*) for four variables and indicate that (i) the maximum permitted value of $\epsilon$ for an accurate solution decreases as $\beta$ increases (this

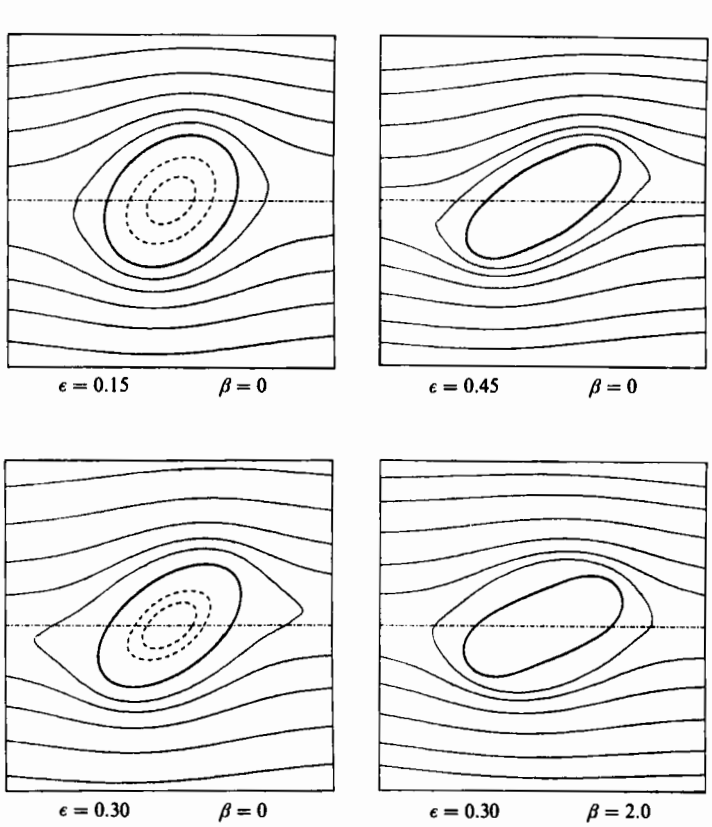


FIGURE 4. Streamline patterns and membrane shapes for several values of $\epsilon$ and $\beta$.

is true for all variables), and (ii) at a given $\epsilon$ and $\beta$ the viscous stress and pressure (which depend on higher derivatives of the stream function) are generally less accurate than the membrane shape and tension. Without the conformal transformation the accuracy-limiting values of $\epsilon$ would be much smaller – for example, for the tension $\epsilon$ would have to be less than 0.30 (versus 0.45) to achieve comparable accuracy with $\beta = 0$. All the results presented in the next section were computed from the conformally transformed expansions equations (56), and we have usually stayed within the limits indicated by figure 3 (*c*), so that the results displayed can be expected to agree with the exact solution to within graphical accuracy.

## 6. Results

Typical streamline patterns and deformed membrane shapes are shown in figure 4. The membrane deformation increases rapidly with increasing dimensionless shear rate, $\epsilon$, attaining an aspect ratio of about 2.5 when $\epsilon = 0.45$. The influence of the viscosity ratio $\beta$ on the streamline pattern is not strong but nevertheless a sufficiently large change in $\beta$ can produce marked changes in the membrane shape, as a comparison of the two lower graphs of figure 4 will confirm. No interior streamlines are shown in the two right-hand graphs of figure 4 because the un-transformed interior solution is not accurate for such large membrane deformations. Isobars of interior and exterior pressure are shown in figure 5. Both inside and outside the membrane there are two pockets where the pressure is above average and two where

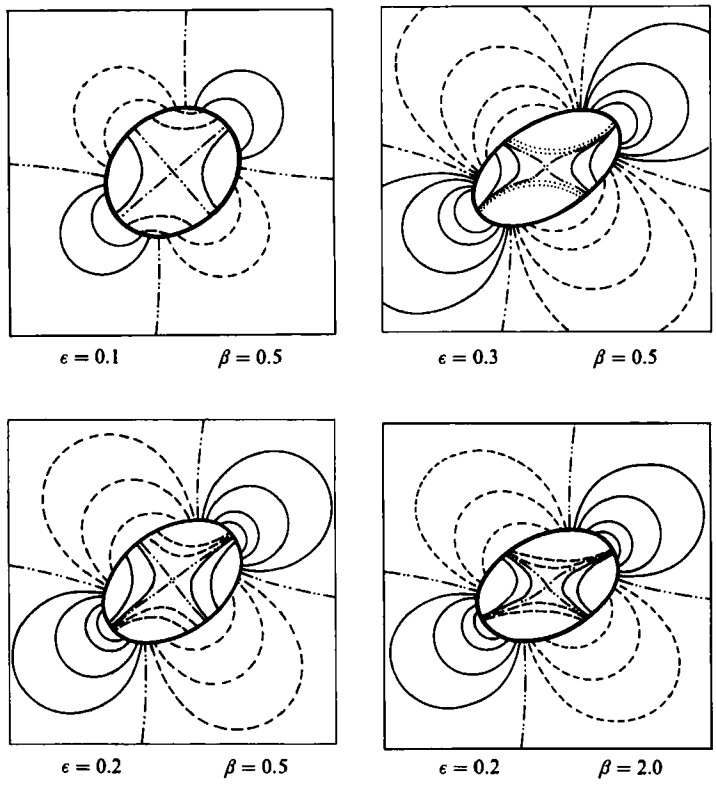


FIGURE 5. Isobars of the external and internal pressure fields for several values of $\epsilon$ and $\beta$. In the exterior flow solid and dashed curves indicate, respectively, positive and negative pressures; the pressure values are $p = \pm 0.05, \pm 0.10, \pm 0.20, \pm 0.30$, with $p = \pm 0.05$ being the pressure on the isobars furthest from the membrane. In the interior flow the solid and dashed curves indicate, respectively, pressures above and below $p = 1$; the pressure values are $p = 1 - 0.006, 1 - 0.012, 1 + 0.003, 1 + 0.014$, with the first and third of these closest to the centre. (The dotted internal isobars at $\epsilon = 0.2$ and $\beta = 2.0$ are extrapolated, as they could not be computed accurately from the untransformed interior expansion with these parameter values.)

it is below average. The peaks and troughs of the exterior pressure occur at the points of minimum and maximum membrane curvature, whereas the peaks and troughs of the interior pressure occur about midway between these points of extreme curvature.

The variation of the membrane tension, $T$, along the membrane as a function of $\epsilon$ and $\beta$ is shown in figure 6; the tension varies strongly with $\epsilon$ and weakly with $\beta$. The minimum tension occurs near the point of maximum membrane curvature and *vice versa*. Figure 7 (*b*) shows the exterior pressure, ${}^{e}p$, along the membrane. This is a strong function of $\epsilon$ but a very weak function of $\beta$, and to a first approximation the exterior pressure resembles the membrane tension. The interior pressure was computed from the conformally-transformed membrane tension and exterior pressure via the boundary condition (15), and is shown in figure 7 (*a*). Within the range of validity of our solution the interior pressure varies only weakly with both $\epsilon$ and $\beta$. The interior and exterior viscous shear stresses on the membrane are shown respectively in figure 8 (*a*) and 8 (*b*). The exterior shear stress is comparable to the exterior and interior pressures, but the interior shear stress remains very small for all values of $\epsilon$ and $\beta$ where our solution is accurate.

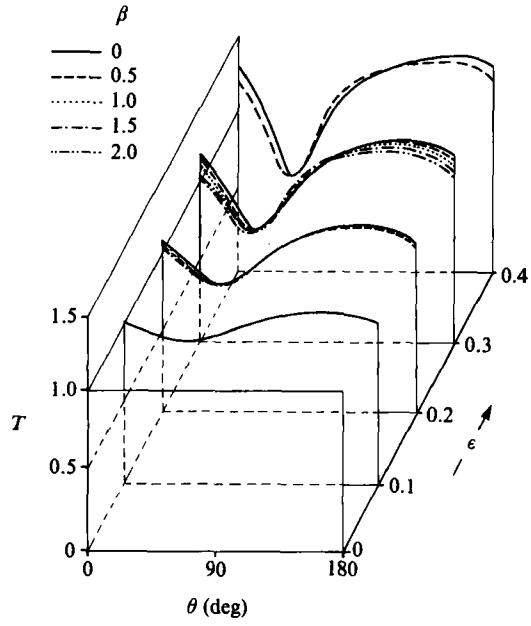


FIGURE 6. Membrane tension as a function of angular position for several values of $\epsilon$ and $\beta$.

Finally, figures 9 and 10 show the dependences of some global characteristics on $\epsilon$ and $\beta$. In the upper part of figure 9 the aspect ratio, $(r_{\max}/r_{\min})$, of the deformed membrane is plotted as a function of $\epsilon$ for various constant values of $\beta$. The deformation increases somewhat faster than linearly with $\epsilon$, and at sufficiently large values of $\epsilon$ also increases with $\beta$. The expanded scale inset to this graph shows, however, that for low values of $\epsilon$ the deformation actually decreases with $\beta$ – but this effect is small. Figure 9(*b*) shows that the major axis of the deformed membrane rotates toward the horizontal as $\epsilon$ increases at constant $\beta$; this angle of inclination also decreases if $\beta$ is increased at constant $\epsilon$ – that is, as the interior becomes more viscous relative to the exterior. In figure 10(*a*) we have plotted the tangential component of the external velocity on the membrane for $\beta = 0$, as a function of position for several values of $\epsilon$.† The boundary conditions require that this speed be constant, and it is so for sufficiently low $\epsilon$; at $\epsilon = 0.3$ fluctuations appear and increase rapidly with increasing $\epsilon$, indicating a breakdown in convergence of the velocity expansions, but even at $\epsilon = 0.4$ the root-mean-square deviation of the computed surface speed from its mean value is less than 15% of the mean. The arclength-averaged surface speeds are shown, as functions of $\epsilon$ and $\beta$, in figure 10(*b*), and these speeds agree with (54) if $\epsilon$ is not too high. It can be seen that the dimensionless surface

† This tangential velocity component was actually computed as follows:

Using (23) we can write the membrane velocity in terms of its tangential and normal components as $v_n - \mathrm{j}v_s = -\mathrm{e}^{-\mathrm{j}\omega}(\phi + z\overline{\phi}' + \overline{\chi}')$ where $\omega$ is the argument of $(\mathrm{d}z/\mathrm{d}\alpha) = (\mathrm{d}z/\mathrm{d}\zeta)(\mathrm{d}\zeta/\mathrm{d}\alpha)$ on the membrane. First, the conformal mapping, (55), was used to transform the expression in parentheses on the right-hand side of the above equation for the membrane velocity to a function of $\zeta$ and $\epsilon$, and the result was expanded and truncated at $O(\epsilon^5)$. Then $\zeta$ on the membrane was taken as $\rho(\alpha)\,\mathrm{e}^{\mathrm{j}\alpha}$, with $\rho(\alpha)$ given by (59); this $\zeta$ was inserted into the truncated velocity formula, and also used to compute $\omega$ as a function of $\alpha$ on the membrane, which was also inserted into this formula. The imaginary part of the resulting expression is plotted as the tangential velocity on the membrane in figure 10(*a*).

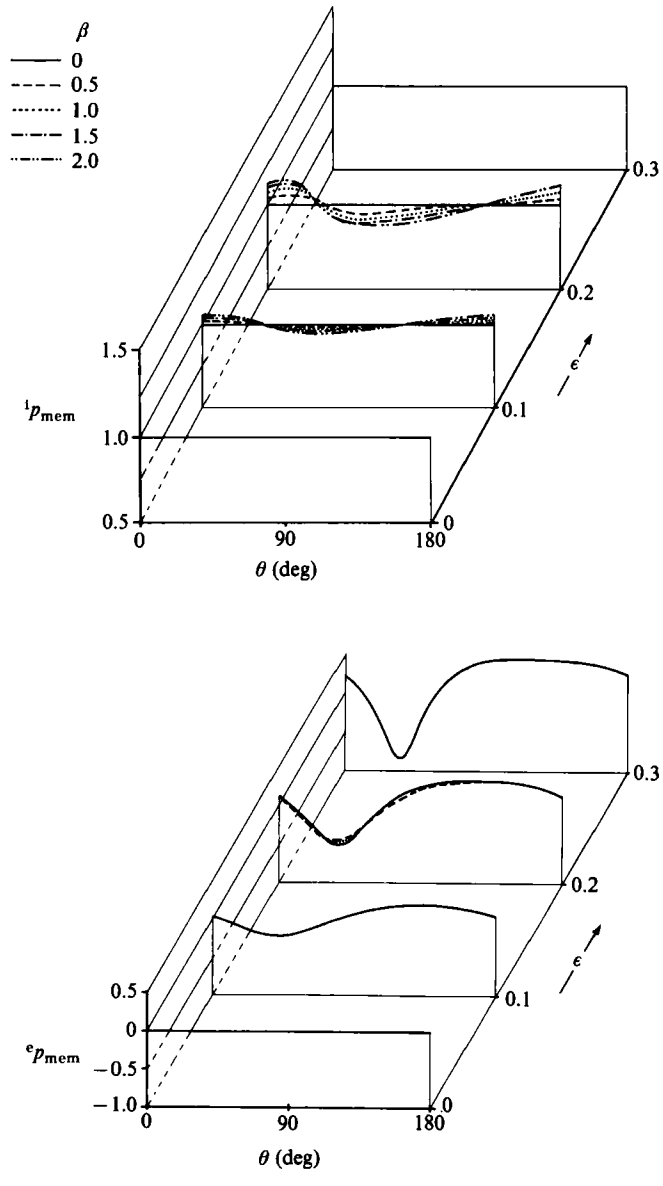


FIGURE 7. Internal and external pressure on the membrane as a function of angular position for several values of $\epsilon$ and $\beta$. The internal pressure is computed from (15).

speed increases somewhat less than linearly with $\epsilon$ at constant $\beta$, and decreases with $\beta$ at constant $\epsilon$.

## 7. Discussion

In this study of a tank-treading cylindrical membrane we have retained the major advantage of classical perturbation analysis while simultaneously mitigating to a large extent the major disadvantage of this technique. The major advantage retained is that no compromises or *a priori* assumptions need be made in the formulation of

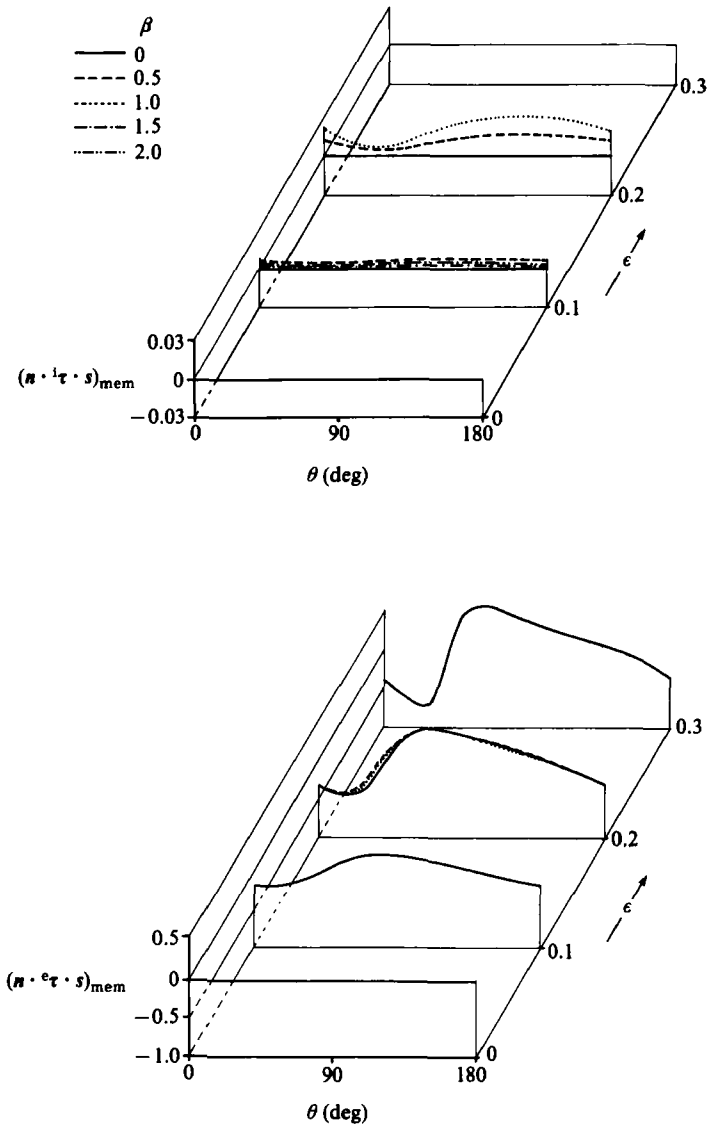


FIGURE 8. Internal and external shear stress on the membrane as a function of angular position for various values of $\epsilon$ and $\beta$. The interior shear stress was calculated from (16).

the problem – all for complex physically relevant boundary conditions have been imposed. The major disadvantage which we have overcome by a combination of computer algebra and coordinate transformation is the usually restricted validity of such analyses to rather small deformation. Our analytical results appear to be accurate for quite large deformations – an aspect ratio of about 2.5 for the membrane shape and (exterior) stream function, and an aspect ratio of about 2 for the stresses. Perhaps the major value of the additional terms obtained by computer algebra is that they have permitted a rational assessment of the accuracy of the perturbation solution. In contrast, an examination of the three-dimensional first-order perturbation solution for liquid droplets by Cox (Cox 1968) and the second-order solution for elastic capsules by Barthes-Biesel (Barthes-Biesel 1980) show that the membrane

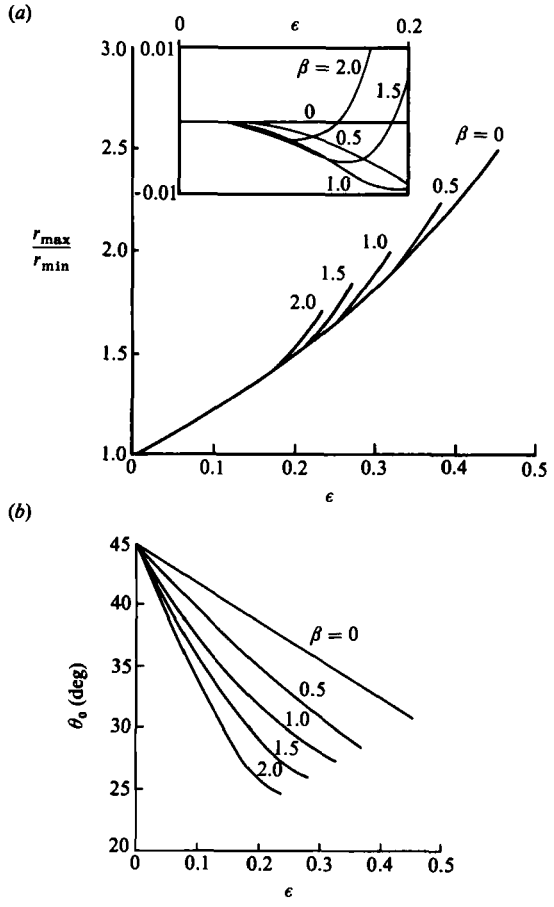


FIGURE 9. (*a*) Aspect ratio of the deformed membrane as a function of $\epsilon$ and $\beta$. The inset shows versus $\epsilon$ on an expanded scale the *differences* $(r_{max}/r_{min})-(r_{max}/r_{min})_{\beta=0}$, in aspect ratios at several values of $\beta$ and the aspect ratio at $\beta = 0$. (*b*) Angle of inclination of the major axis of the deformed membrane to the horizontal (i.e. remote zero-velocity plane) direction, as a function of $\epsilon$ and $\beta$.

shapes yielded by both these analyses develop negative curvature at an aspect ratio of about 1.5, as does our untransformed solution if it is truncated at $O(\epsilon^2)$. This reversal of membrane curvature is a mathematical artifact, as it can be eliminated by retaining more terms in the series; for aspect ratios greater than 1.5 the predicted cross-sections of the membrane resemble 'dumb-bells' and the associated solutions can no longer be assumed accurate. Of course, the analyses of Cox and Barthes-Biesel are of three-dimensional problems and therefore inherently much more complex than the two-dimensional problem we have considered.

Published numerical studies of the tank-treading problem have been two-dimensional and have invariably assumed that the membrane is an ellipse of given aspect ratio and orientation (Sugihara & Niimi 1984; Niimi & Sugihara 1985). Figure 4 shows, however, that the membrane cross-section may be markedly non-elliptic – for example when $\epsilon = 0.3$ and $\beta = 2.0$. This probably does not affect the gross streamline pattern very much, but it could lead to substantial errors in variables like the membrane tension which are strongly affected by the membrane curvature. In our approach one need not – indeed, one cannot – make *a priori* assumptions about

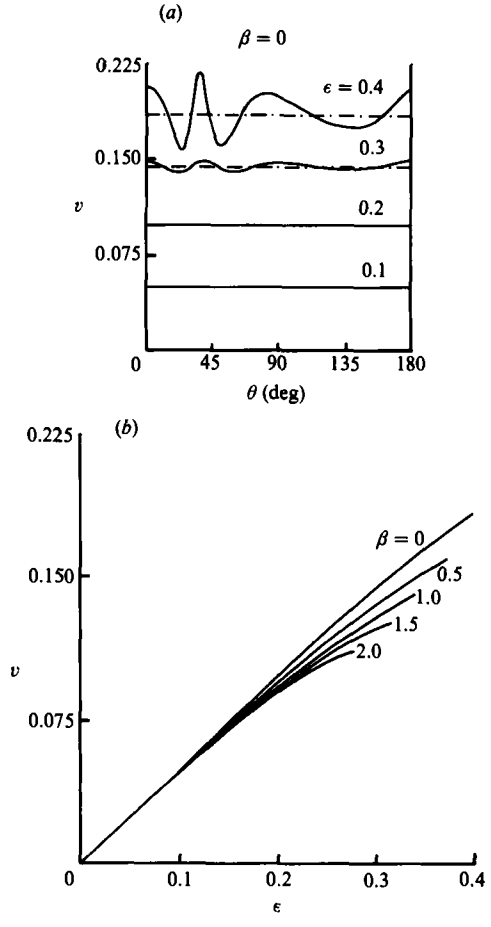


FIGURE 10. (*a*) Tangential component of the external velocity on the membrane, given by the transformed expansion as a function of angular position for several values of $\epsilon$ with $\beta = 0$. The dashed lines are averages (weighted by arc length) of the tangential velocity (surface speed). (*b*) Average surface speed as a function of $\epsilon$ and $\beta$.

membrane shape, orientation, and speed, as all this information is provided by the solution.

Our main concern in this paper was to establish and validate a method of analysis for a class of problems, and therefore we have chosen what is probably the simplest problem in this class: the inextensible membrane. Inextensibility has required that we specify the pressure at the centre of the membrane in order to determine the interior pressure uniquely. This condition is somewhat artificial in the context of the physical problems which motivated this study, but it probably has no important impact on the utility of the analytical method or the significance of the results. Rao has constructed the series solution to the problem of a pressurized elastic, rather than inextensible, cylinder (Rao 1985) up to $O(\epsilon^2)$ and has found – not unexpectedly – that this solution closely resembles the one presented in this paper. Further, many aspects of our solution agree, at least qualitatively, with results reported by Barthes-Biesel for a spherical elastic capsule, including an increase in tank-treading frequency with shear-rate, a concomitant tilting of the major axis toward the shear planes, and an increase of the aspect ratio of the deformed membrane with shear rate and viscosity

ratio, $\beta$. (She does not mention a decrease of the deformation with increasing $\beta$ at low shear rates, as shown in the inset to figure 9(*a*).) Barthes-Biesel finds no effect on $\beta$ on the tank-treading frequency, and this is probably because in her problem as in ours (see (54)) this effect first appears in terms of $O(\epsilon^3)$, whereas her expansions do not go beyond $O(\epsilon^2)$.

The results presented herein demonstrate that classical perturbation techniques combined with computer algebra offer an attractive alternative to purely numerical approaches for solving certain types of difficult nonlinear large-deformation problems. Our analytical technique and two-dimensional model permits a very detailed examination of the streamlines, velocities, and stresses. Once the basic solution algorithm has been programmed it requires but minor modifications to account for various alternative membrane properties, including nonlinear viscoelasticity and bending rigidity. We have several of these problems under study and the results will be reported in due course.

This work was supported by Grant HL-12839 from the National Heart, Lung and Blood Institute, US Public Health Service.

## REFERENCES

BARTHES-BIESEL, D. 1980 Motion of a spherical microcapsule freely suspended in a linear shear flow. *J. Fluid Mech.* **100**, 831–853.

BARTHES-BIESEL, D. & SGAIER, H. 1985 Role of membrane viscosity in the orientation and deformation of a spherical capsule suspended in shear flow. *J. Fluid Mech.* **160**, 119–135.

COX, R. G. 1968 The deformation of a drop in a general time-dependent fluid flow. *J. Fluid Mech.* **37**, 601–623.

DUFF, G. D. F. & NAYLOR, D. 1966 *Differential Equations of Applied Mathematics*, p. 143. Wiley.

KELLER, S. R. & SKALAK, R. 1982 Motion of a tank-treading ellipsoidal particle in a shear flow. *J. Fluid Mech.* **120**, 27–47.

KHOLIEF, I. A. & WEYMANN, H. D. 1974 Motion of a single red blood cell in a plane shear flow. *Biorheology* **11**, 337–348.

KOBER, H. 1957 *A Dictionary of Conformal Representations*, p. 177. Dover.

LANGLOIS, W. E. 1964 *Slow Viscous Flows*. Macmillan.

MUSKHELISHVILI, N. I. 1953 *Some Basic Problems of the Mathematical Theory of Elasticity*. Groningen-Holland: P. Noordhoff.

NIIMI, H. & SUGIHARA, M. 1985 Cyclic loading on the red cell membrane in a shear flow: a possible cause of hemolysis. *J. Biomech. Engng* **107**, 91–95.

RAND, R. H. 1984 *Computer Algebra in Applied Mathematics: An Introduction to MACSYMA*. Boston: Pittman.

RAO, P. R. 1985 Deformation of a fluid-filled cylindrical membrane by a slow viscous shear flow. M.S. thesis, Department of Mechanical Engineering, Washington University, St Louis.

SCHMID-SCHÖNBEIN, H. & WELLS, R. E. 1969 Fluid drop like transition of erythrocytes under shear stress. *Science* **165**, 288–291.

SUGIHARA, M. & NIIMI, H. 1984 Numerical approach to the motion of a red blood cell in Couette flow. *Biorheology* **21**, 735–749.

SUTERA, S. P. & TRAN-SON-TAY, R. 1983 Mathematical model of the velocity field external to a tank-treading red cell. *Biorheology* **20**, 267–282.

SUTERA, S. P., GARDNER, R. A., BOYLAN, C. W., CARROLL, G. L., CHANG, K. C., MARVEL, J. S., KILO, C., GONEN, B. & WILLIAMSON, J. R. 1985 Age-related changes in deformability of human erythrocytes. *Blood* **65**, 275–282.

TAYLOR, G. I. 1932 The viscosity of a fluid containing small drops of another fluid. *Proc. R. Soc.* A **138**, 41–48.